Fermionic scenario for the destruction of superconductivity in ultrathin MoC films evidenced by STM measurements

P. Szabó,[1,*] T. Samuely,[1] V. Hašková,[1] J. Kačmarčík,[1] M. Žemlička,[2] M. Grajcar,[2] J. G. Rodrigo,[3] and P. Samuely[1,†]

[1]*Centre of Ultra Low Temperature Physics, Institute of Experimental Physics, Slovak Academy of Sciences, and P. J. Šafárik University, SK-04001 Košice, Slovakia*

[2]*Department of Experimental Physics, Comenius University, SK-84248 Bratislava, Slovakia*

[3]*Departamento de Física de la Materia Condensada, Laboratorio de Bajas Temperaturas, Instituto de Ciencia de Materiales, Nicolás Cabrera, Condensed Matter Physics Center, Universidad Autónoma de Madrid, E-28049 Madrid, Spain*

We use sub-Kelvin scanning tunneling spectroscopy to investigate the suppression of superconductivity in homogeneously disordered ultrathin MoC films. We observe that the superconducting state remains spatially homogeneous even on the films of 3-nm thickness. The vortex imaging suggests the global phase coherence in our films. Upon decreasing thickness, when the superconducting transition drops from 8.5 to 1.2 K, the superconducting energy gap Δ follows T_c perfectly. All this is pointing to a two-stage fermionic scenario of the superconductor-insulator transition (SIT) via a metallic state as an alternative to the direct bosonic SIT scenario with a Cooper-pair insulating state evidenced by the past decade STM experiments.

Superconductor-insulator transition (SIT) can be tuned in different ways, e.g., by increasing the physical or chemical disorder, by the change in charge-carrier density, by a magnetic field, etc. Decreasing the superconducting film thickness down to several atomic layers is yet another possibility [1]. Superconductivity is characterized by the order parameter $\Psi = \Delta e^{i\phi(r)}$ with the amplitude Δ and phase ϕ. Two fundamental approaches describe SIT as a consequence of either the quasiparticle fluctuations affecting the amplitude Δ or the phase fluctuations of Ψ. The quasiparticle fluctuations correlate to the fermionic scenario [2,3]. There, disorder-enhanced Coulomb interaction breaks Cooper pairs into fermionic states leading to superconductor-(bad-) metal transition with $\Delta \to 0$ at $T_c \to 0$. At even higher disorder metal-insulator transition (MIT) follows due to Anderson localization. The bosonic scenario [4,5] assumes a direct SIT. On the superconducting side even in a homogeneously disordered system superconducting "puddles" with variant Δ emerge. In the insulating state Cooper pairs with a finite amplitude are still present, but their global phase coherence is lost. A comprehensive review on SIT as a quantum phase transition [6] concludes that many characteristics in both scenarios are very similar, and probably only a probe directly sensitive to the local variations of the superconducting energy gap/order parameter can discern the realized mechanism. The scanning tunneling microscope (STM) is a unique probe with such a capability.

The available STM experiments on thin films of TiN, InO$_x$, and NbN [7–13] bring evidence that upon increasing disorder, Δ decreases more slowly than T_c, the variation of Δ on a scale of the superconducting coherence length ξ increases, a pseudogap appears above T_c in the tunneling spectra, the spectral coherence peaks are suppressed, and the vortex lattice is fading out. This phenomenology strongly supports the bosonic scenario and raises the question about the universality of the bosonic SIT [14]. On the other hand, potential evidence

for the fermionic mechanism was provided even sooner by the tunneling experiments on planar junctions on amorphous Bi and PbBi/Ge films [15,16] indicating that the Cooper pair amplitude vanishes at SIT. But the unambiguousness of these results was challenged by the fact that the spatially averaged tunneling spectra were gapless. This gaplessness could be explained by a very inhomogeneous gap distribution due to phase fluctuations. Then, superconducting pair correlations might also exist in insulators close to SIT, contradicting the fermionic scenario.

Here, we present sub-Kelvin STM experiments on ultrathin superconducting MoC films with atomic spatial resolution. We demonstrate the spatial homogeneity of the superconducting state for film thicknesses down to 3 nm and the closing of the superconducting energy gap/order parameter as T_c vanishes, in agreement with the fermionic scenario. Thus, we bring direct evidence on the local behavior of the superconducting order parameter in this class of the transition.

The MoC films were prepared by the magnetron reactive sputtering from a Mo target in an argon acetylene atmosphere onto a sapphire *c*-cut substrate. The details can be found elsewhere [17]. The preparation followed the procedure of Lee and Ketterson [18] who manufactured continuous MoC films down to 0.4-nm thickness showing the separatrix between the superconducting and the insulating films at 1.3-nm thickness with a sheet resistance R_S of about 2.8 kΩ.

The inset of Fig. 1(a) shows the resistive transitions near T_c on 30-, 10-, 5-, and 3-nm-thick MoC films. The gradual shift of T_c (defined at 50% of R_S above the transition) from 7.3 to 6.7, 3.75, and 1.2 K, respectively, is accompanied by an increase in R_S from several tens of ohms to almost 1400 Ω. The transitions remain sharp while shifting to lower temperatures strongly suggesting that our films are homogeneously disordered [19]. The main part of Fig. 1(a) presents the overall temperature dependence of R_S from room temperature down to the superconducting transition showing a negative derivative dR_S/dT for all the films. Such a behavior can be described within the framework of the quantum corrections [20,21] to the standard Drude conductivity for
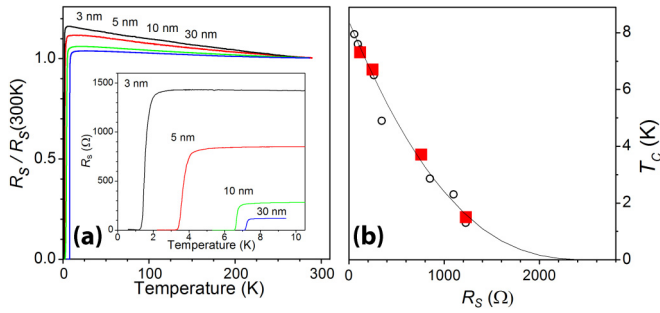
*pszabo@saske.sk
†samuely@saske.sk

FIG. 1. (a) Temperature dependence of the sheet resistance R_S normalized to its value at $T = 300$ K for 3-, 5-, 10-, and 30-nm MoC films. The inset: R_S near T_c. (b)The critical temperature T_c as a function of the sheet resistance R_S for the measured films (squares) and other series (circles), and the solid line is Finkelstein's fit.

disordered metals (weak localization and electron-electron interactions). These corrections are rather weak bringing about

a 15% increase in R_S before the thinnest 3-nm MoC film goes superconducting. Figure 1(b) shows a dependence of T_c on R_S (the latter measured at 300 K) for the films used in the STM measurements (red squares) supplemented by another series of MoC films (circles). The solid line is a fit to Finkelstein's model [3] indicating termination of superconductivity at $R_{cr} \approx 2.5$ kΩ close to the value determined in Ref. [18]. Magnetotransport and Hall-effect measurements allowed for the determination of the superconducting coherence length ξ which increases from 5 to 8 nm and the Ioffe-Regel product of $k_F l$ dropping from 5 to 1.3 when the thickness of the MoC film is diminished from 30 to 3 nm. Notably the carrier density is very high $n \approx 10^{23}$ cm^{-3} and not changing [22].

The STM and scanning tunneling spectroscopy (STS) experiments were performed by means of a sub-Kelvin STM system developed in Košice enabling measurements above $T = 280$ mK and magnetic fields up to $B = 8$ T. Prior to STM experiments a protective layer on the surface of the films has been dissolved and the samples mounted within few minutes
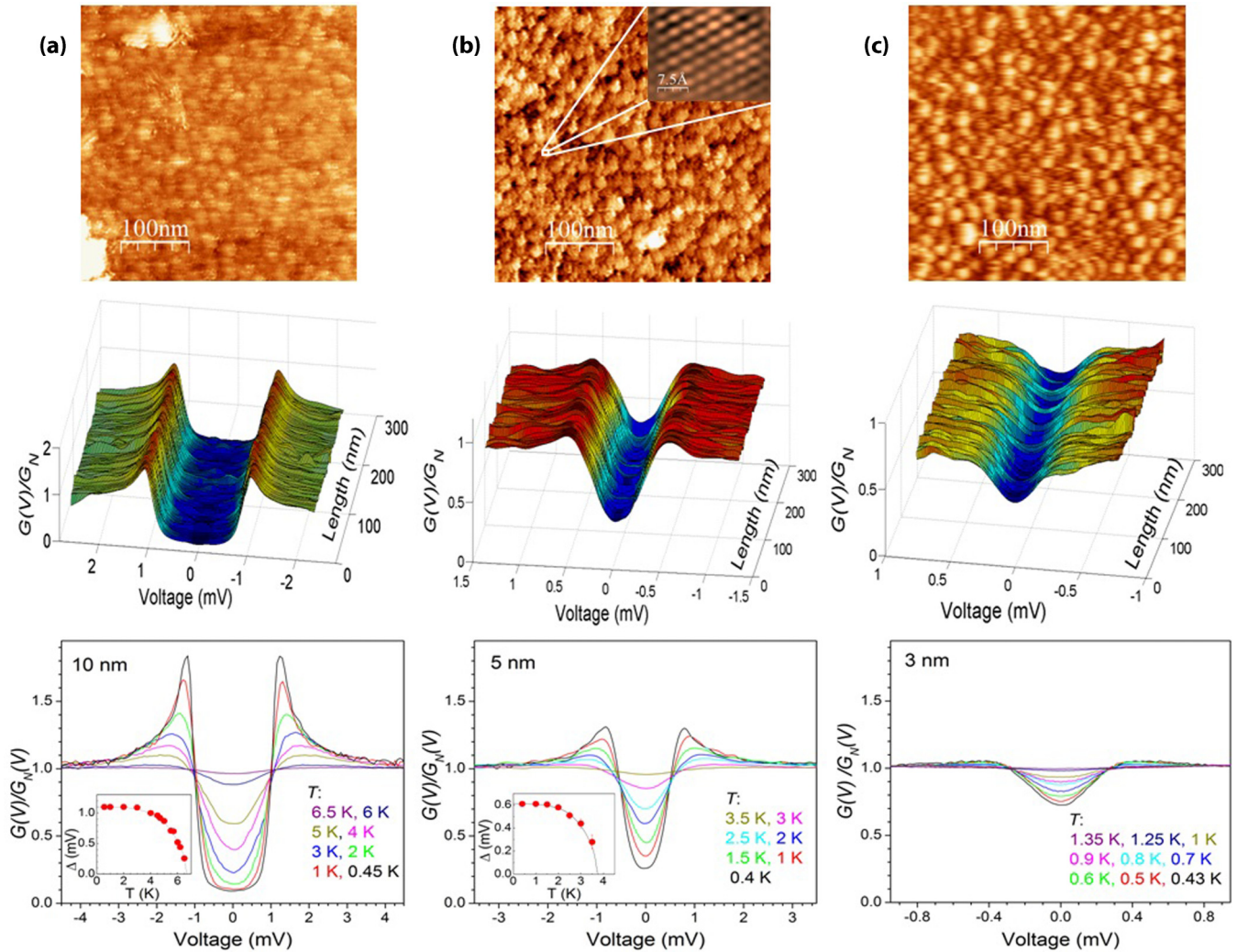

FIG. 2. STM surface topography and locally measured tunneling spectra for 10-, 5-, and 3-nm MoC films (a)–(c), respectively. Top: STM surface topographies at 500 mK, zoom in 5-nm film shows atomic structure. Middle: 100 STS spectra along an ∼200-nm line on the surface of the respective film taken at 450 mK. Bottom: Temperature dependence of a typical tunneling spectrum at indicated temperatures. The insets of (a) and (b): Temperature dependence of the gap determined from fits to Dynes formula (points) and BCS-like $\Delta(T)$ dependence (line).

to the ^{3}He cryostat. Surface topography has been performed in the constant current mode. Conductance maps and vortex imaging have been studied via the current imaging tunneling spectroscopy mode [23] in a 128×128 grid.

The surface topography measurements have been realized on all our thin films at tunneling resistances in the range of 50–100 MΩ. The top panels of Fig. 2 show topographic images of 400×400 nm^2 surfaces obtained on 10-, 5-, and 3-nm films (a)–(c), respectively at $T = 450$ mK. Our films show clean surfaces, revealing a compact polycrystalline structure with the lateral grain size of $\sim$15–30 nm. Given the sharp superconducting transitions the grain boundaries are very transparent. A rms roughness of the films was typically 0.6–0.7 nm in agreement with the topography obtained by atomic force microscope [22]. A zoom of a 3×2.5 nm^2 area is displayed in the topography of the 5-nm film (inset in the topography image), showing atomically resolved surfaces with a distorted hexagonal crystal symmetry [24,25], which allow for correlated topographic (STM) and spectroscopic (STS) studies. It also proves that grains are single nanocrystals.

The tunneling conductance curves $G(V,x,y) = dI(V,x,y)/dV$ vs V are calculated by numerical differentiation of the locally measured I-V characteristics. Since the metallic Au tip features a constant density of states at the measured bias energies, each of the differential conductance vs voltage spectra reflects the superconducting density of states (SDOS) of the MoC films, smeared by $\sim \pm 2\, k_B T$ in energy at the respective temperature. Consequently, in the low-temperature limit, the differential conductance measures directly the SDOS. The three-dimensional plots shown in the middle panels of Fig. 2 display three series of 100 tunneling spectra $G(V,x,y)$ taken along 200–250-nm lines at $T = 450$ mK on the 10-, 5-, and 3-nm MoC films. The spectra are normalized to the conductance values G_N at $eV = 4\Delta$ above the gap energies. In the 10-nm films, the spectra show a pronounced superconducting structure with well-defined coherent peaks near the gap energies at $V \sim \pm \Delta/e$ without any significant spatial variation across the sample surface. Notably, we always observed a finite conductance inside the gap region with a value at zero bias $G(V = 0,x,y)$ of around 0.1 G_N. This is not compatible with a pure BCS SDOS considering the thermal smearing at 450 mK. We address this phenomenon below but note that the complex conductivity derived from our recent experimental transmission measurements on coplanar waveguide resonators made of 10-nm MoC film shows a finite quasiparticle lifetime consistent with the existence of in-gap quasiparticle states [26].

The series taken on the 5-nm film reveals gaplike features with coherent peaks located at a smaller bias (mean value of the peak position is $V = 0.88$ mV with $\sigma = 0.022$ mV) as expected for a sample with lower T_c, but the height of the peaks is significantly smaller than in the case of the 10-nm film. Moreover, the intensity of the in-gap states is substantially increased to a value of $G(V = 0,x,y)$ around 0.3G_N. This tendency continues on the 3-nm MoC film where the series of spectra features a reduced tunneling conductance around the zero-bias voltage and the in-gap states bring the value of $G(V = 0,x,y)$ to around 0.7 G_N and almost no signatures of coherence peaks. Moreover, a quasilinearly increasing
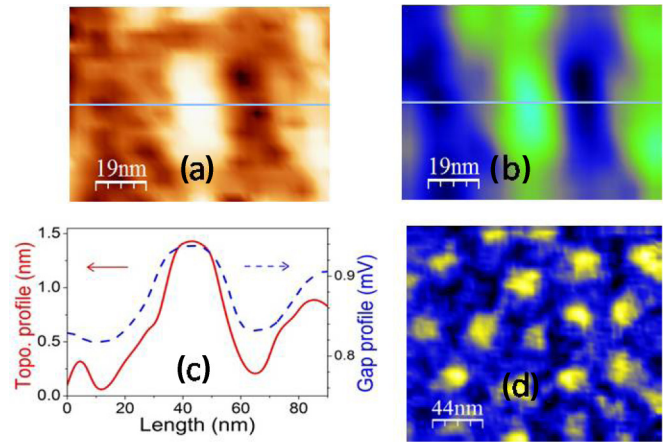

FIG. 3. (a) STM topography on a 5-nm MoC film showing protruding grain as a white spot. (b) Gap map of the same area taken at $T = 450$ mK. (c) Profiles of topography (full curve) and gap map (dashed curve) along the gray lines in (a) and (b). (d) Vortex image on a flat surface of the 5-nm MoC film at 450 mK in $B = 1$ T showing 21 vortices.

background of the tunneling conductance at higher-bias voltages is present. The latter finding indicates an appearance of the Altshuler-Aronov effect of suppression of density of states due to a disorder-enhanced Coulomb interaction [20].

For the different particular film thicknesses we analyzed numerous series of spectra, such as the ones presented in Fig. 2. None of them show any characteristic length scale of variations which would indicate emerging superconducting granularity, such as, e.g., in TiN [7]. On the contrary, the same variations are found independently on a bias voltage for spectra taken along lines with a step size of 2 nm (Fig. 2) or, e.g., 0.05 nm (not shown). In the conductance maps (recorded at zero bias or at biases close to the gap value) on all studied MoC films, a variation with the same standard deviation of about 0.05 in normalized conductance is found. As such, these variations result from the noise of the apparatus rather than physical properties of the superconducting films. This implies a high spatial homogeneity of superconductivity in MoC.

Figures 3(a)–3(c) present a surface analysis performed on another 5-nm MoC film. In (a) the STM surface topography of a small area of 95×65 nm^2 shows a protruding grain (white spot). Figure 3(b) displays the gap map (bias voltage of coherence peaks) of the same area taken at $T = 450$ mK, and (c) provides the topography (red curve—left scale) and the gap map (blue curve—right scale) along the gray lines in (a) and (b). On the grain where the film is thicker a larger gap is found, notably in an area of size much larger than the superconducting coherence length $\xi \approx 8$ nm. From these data it is evident that the only systematic change in the gap value in our MoC films is due to the change in their thicknesses and that the superconducting state remains spatially homogeneous on all MoC films with constant thicknesses. This is very different from the STS measurements on TiN, InO$_x$, and NbN thin films showing an emergent granularity in the superconducting condensate upon increasing disorder on the scale of the coherence length [7,9,12,13].

Figure 3(d) shows a zero-bias conductance map obtained on the 5-nm film on a flat surface of 220×190 nm^2 at $T = 450$ mK in a magnetic field of $B = 1$ T. A distorted vortex lattice is observed. At 1 T, the average intervortex distance for the triangular Abrikosov lattice $d_v = 1.075(\Phi_0/B)^{1/2}$ is about 50 nm, resulting in some 21 vortices for an area equivalent to the one in the figure, as we actually find in our measurement. We have observed the presence of vortices in MoC films down to 5 -nm thickness. In the case of 3 nm the low contrast between the superconducting and normal spectra prevents vortex imaging. The presence of vortices in MoC brings evidence for a global phase coherence in the samples allowing for supercurrent flow around the vortex cores.

The bottom panels of Fig. 2 show the effect of temperature on the tunneling spectra normalized to the tunneling curves $G_N(V)$ measured in the normal state above T_c. $G_N(V)$ of the 10- and 5-nm films were constant in the presented bias voltage range whereas on the 3-nm film a weak V-shaped normal state is present fitting the background shown in Fig. 2(c), middle panel. The local T_c's have been established from the STS data as the temperatures where superconducting features disappear. Then, T_c's are 6.7, and 3.7, and 1.2–1.25 K for the 10-, 5-, and 3-nm films, respectively, in agreement with the transport data (see Fig. 1). No indications of a pseudogap featuring a reduced DOS above the bulk T_c have been observed. We have measured five to ten temperature dependencies on all our films taken at different locations, but no variations of the local T_c on a particular film have been observed. It again supports the spatial homogeneity of the superconductivity of the MoC films.

To fit our spectra with finite in-gap states the Dynes modification of the BCS density of states $N(E) = Re\{E/(E - \Delta)^{(1/2)}\}$ where the complex energy $E = E' + i\Gamma$ with a smearing parameter Γ has been taken into account [27]. The temperature dependencies of Δ have been determined from fits to the thermally smeared Dynes formula on the 10- and 5-nm films. The large smearing effect in the 3-nm film prevented reliable fits at higher temperatures. The resulting $\Delta(T)$ dependencies presented in the insets of the bottom panels of Fig. 2 follow the predictions of the BCS theory (solid lines). In the fits Γ is found to be temperature independent up to $\sim 0.5\,T_c$, whereas at higher temperatures it is increased up to $\sim 4\Gamma(0)$ at T_c.

The tunneling spectra at $T = 450$ mK (solid lines) together with the Dynes fits (open symbols) are resumed in Fig. 4(a). There we have also included the result for the 30-nm-thick MoC film which displays a hard spectral gap with a flat zero tunneling conductance in a finite range of bias voltages inside the gap region. The fit provides $\Delta(0) = 1.23$ meV with $\Gamma = 0$ fully in line with the BCS theory. The observation of the hard gap here proves that the spectral smearing on the other samples is not due to a lack of energy resolution. As sample thickness is decreased, the inferred gap/order parameter $\Delta(0)$ is decreased in a sequence $\Delta(0) = 1.1$, 0.62, and 0.2 meV for the 10-, 5-, and 3-nm film thicknesses, respectively. As presented in Fig. 4(b) the thickness dependence of the superconducting gap Δ (red squares) perfectly follows the thickness dependence of the transition temperature T_c (circles). Figure 4(c) shows that the superconducting coupling ratio $2\Delta/k_B T_c$ remains constant and being equal to about 3.8 for all the studied MoC films.
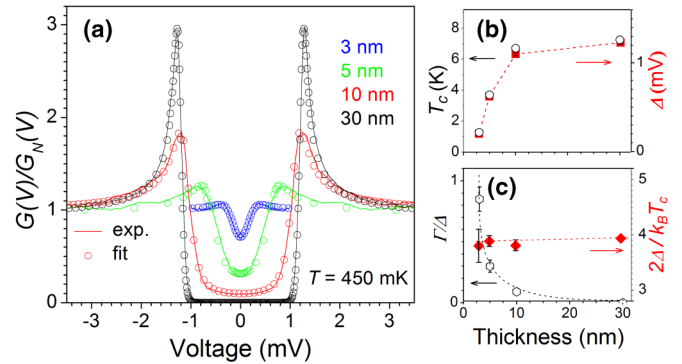

FIG. 4. (a) Typical tunneling conductances of the 3-, 5-, 10-, and 30-nm thin MoC films at $T = 450$ mK—solid lines. The symbols are fits to the thermally smeared Dynes formula. (b) Film thickness dependence of the superconducting energy gap (red solid symbols—right scale) and of the critical temperature determined from tunneling experiment (open circles—left scale). (c) Film thickness dependence of the Dynes smearing parameter normalized to the gap—Γ/Δ at $T = 450$ mK (open circles—left scale) and of the superconducting coupling strength $2\Delta/k_B T_c$ (red solid diamonds—right scale).

All this strongly suggests that superconductivity is suppressed ($T_c \rightarrow 0$) when $\Delta \rightarrow 0$.

We can now compare our findings with the bosonic SIT phenomenology found in the STS experiments on TiN, InO$_x$, and NbN films [7–13]. In contrast to those experiments we have found that upon increasing disorder, Δ decreases in the same way as T_c, there are no spatial variations of Δ, and no pseudogap above T_c appears. Also, the vortex lattice is present. In the strongly disordered MoC films the spectral coherence peaks are suppressed but in a different way than, for example, in InO$_x$ [10]. In MoC their suppression is correlated with the increase in the in-gap states which can be quantitatively accounted for by the increasing relative strength of the Dynes parameter normalized to the zero-temperature gap value Γ/Δ. Figure 4(c) shows a steep increase in this parameter from zero (30-nm film) to 0.9 for the 3-nm film.

As mentioned above, broadened SDOS have already been observed on other films near SIT. Valles *et al.* found heavily broadened SDOS in planar tunnel junctions made on ultrathin Bi film with $T_c = 0.7$ K [15] but also on the series of ultrathin PbBi/Ge films [16] where it was attributed to spatial variations of the amplitude of the order parameter. In the PbBi films the broadening increases as T_c decreases with maximum $\Gamma/\Delta \sim 0.4$ for $T_c = 0.96$ K. Our spatially homogeneous spectra clearly demonstrate that the origin of the broadening is not the uneven distribution of the gap amplitude. Hence, although the source of the in-gap states remains unclear [28], our findings unequivocally corroborate the fermionic scenario.

The recent measurements of the Little-Park oscillations in the magnetoresistance on uniform a-Bi films with nanohoneycomb arrays of holes also support the fermionic SIT [29]. Then, a question arises what physical parameter decides on the insulating ground state upon the SIT, fermionic, or Cooper-pair insulating one. The MoC superconductors differ from TiN, InO$_x$, and NbN, for example, by the fact that the quantum corrections to the resistivity are small and the charge-carrier

density is high and not changing upon increasing disorder. If these are important ingredients for fermionic scenario, it remains for further studies.

In conclusion, STM and STS studies on ultrathin MoC films provide evidence that, in contrast to TiN, InO$_x$, and NbN where the bosonic scenario of SIT is found in the ultrathin MoC films the superconducting energy gap or order parameter terminates ($\Delta \to 0$) as the bulk superconductivity ceases with $T_c \to 0$, the global superconducting coherence in MoC films is manifested by the presence of superconducting vortices, and most importantly, the superconducting state is very homogeneous for all the thicknesses down to 3 nm where the superconducting transition is suppressed from bulk $T_c = 8.5$ K to 1.3 K and the strong disorder is characterized by $k_F l$ close to unity. All these observations point to the fermionic

route of the SIT confirming that there are at least two different scenarios of SIT that can be realized depending on the physical parameters of the systems.

[1] D. B. Haviland, Y. Liu, and A. M. Goldman, Onset of Superconductivity in the Two-Dimensional Limit, Phys. Rev. Lett. **62**, 2180 (1989).

[2] S. Maekawa, and H. Fukuyama, Localization effects in two-dimensional superconductors, J. Phys. Soc. Jpn. **51**, 1380 (1981).

[3] A. M. Finkel'stein, Superconducting transition temperature in amorphous films, JETP Lett. **45**, 46 (1987).

[4] M. P. A. Fisher, Quantum Phase Transitions in Disordered Two-Dimensional Superconductors, Phys. Rev. Lett. **65**, 923 (1990).

[5] V. J. Emery, and S. A. Kivelson, Importance of phase fluctuations in superconductors with small superfluid density, Nature (London) **374**, 434 (1995).

[6] V. F. Gantmakher and V. T. Dolgopolov, Superconductor-insulator quantum phase transition, Phys.-Usp. **53**, 1 (2010).

[7] B. Sacépé, C. Chapelier, T. I. Baturina, V. M. Vinokur, M. R. Baklanov, and M. Sanquer, Disorder-Induced Inhomogeneities of the Superconducting State Close to the Superconductor-Insulator Transition, Phys. Rev. Lett. **101**, 157006 (2008).

[8] B. Sacepé, C. Chapelier, T. I. Baturina, V. M. Vinokur, M. R. Baklanov, and M. Sanquer, Pseudogap in a thin film of a conventional superconductor, Nat. Commun. **1**, 140 (2010).

[9] Y. Noat, V. Cherkez, C. Brun, T. Cren, C. Carbillet, F. Debontridder, K. Ilin, M. Siegel, A. Semenov, H.-W. Hübers, and D. Roditchev, Unconventional superconductivity in ultrathin superconducting NbN films studied by scanning tunneling spectroscopy, Phys. Rev. B **88**, 014503 (2013).

[10] B. Sacépé, T. Dubouchet, C. Chapelier, M. Sanquer, M. Ovadia, D. Shahar, M. Feigelman, and L. Ioffe, Localization of preformed Cooper pairs in disordered superconductors, Nat. Phys. **7**, 239 (2011).

[11] M. Mondal, A. Kamlapure, M. Chand, G. Saraswat, S. Kumar, J. Jesudasan, L. Benfatto, V. Tripathi, and P. Raychaudhuri, Raychaudhuri, Phase Fluctuations in a Strongly Disordered s-Wave NbN Superconductor Close to the Metal-Insulator Transition, Phys. Rev. Lett. **106**, 047001 (2011).

[12] M. Chand, G. Saraswat, A. Kamlapure, M. Mondal, S. Kumar, J. Jesudasan, V. Bagwe, L. Benfatto, V. Tripathi, and P. Raychaudhuri, Phase diagram of the strongly disordered s-wave

superconductor NbN close to the metal-insulator transition, Phys. Rev. B **85**, 014508 (2012).

[13] A. Kamlapure, T. Das, S. C. Ganguli, J. B. Parmar, S. Bhattacharyya, and P. Raychaudhuri, Emergence of nanoscale inhomogeneity in the superconducting state of a homogeneously disordered conventional superconductor, Sci. Rep. **3**, 2979 (2013).

[14] N. Trivedi, in *Conductor Insulator Quantum Phase Transitions*, edited by V. Dobrosavljevic, N. Trivedi, and J. M. Valles, Jr. (Oxford University Press, Oxford, 2012).

[15] J. M. Valles, Jr., R. C. Dynes, and J. P. Garno, Electron Tunneling Determination of the Order-Parameter Amplitude at the Superconductor-Insulator Transition in 2D, Phys. Rev. Lett. **69**, 3567 (1992).

[16] S.-Y. Hsu, J. A. Chervenak, and J. M. Valles, Jr., Magnetic Field Enhanced Order Parameter Amplitude Fluctuations in Ultrathin Films near the Superconductor-Insulator Transition, Phys. Rev. Lett. **75**, 132 (1995).

[17] M. Trgala, M. Žemlička, P. Neilinger, M. Rehák, M. Leporis, Š. Gaži, J. Greguš, T. Plecenik, T. Roch, E. Dobročka, and M. Grajcar, Superconducting MoC thin films with enhanced sheet resistance, Appl. Surf. Sci. **312**, 216 (2014).

[18] S. J. Lee and J. B. Ketterson, Critical Sheet Resistance for the Suppression of Superconductivity in Thin Mo-C Films, Phys. Rev. Lett. **64**, 3078 (1990).

[19] J. M. Valles, Jr., S.-Y. Hsu, R. C. Dynes, and J. P. Garno, Electron tunneling studies of ultrathin films near the superconductor-to-insulator transition, Physica B **197**, 522 (1994).

[20] B. L. Altshuler and A. G. Aronov, Zero bias anomaly in tunnel resistance and electron-electron interaction, Solid State Commun. **30**, 115 (1979).

[21] B. L. Altshuler, A. G. Aronov, and P. A. Lee, Interaction Effects in Disordered Fermi Systems in Two Dimensions, Phys. Rev. Lett. **44**, 1288 (1980).

[22] J. Kačmarčik, P. Szabó, V. Hašková, T. Samuely, M. Kopčík, and P. Samuely (unpublished).

[23] R. J. Hamers, R. M. Tromp, and J. E. Demuth, Surface Electronic Structure of Si (111)-(7×7) Resolved in Real Space, Phys. Rev. Lett. **56**, 1972 (1986).

[24] E. L. Haase, Preparation and characterization of MoC x thin films, J. Low Temp. Phys. **69**, 245 (1987).

[25] C. I. Sathish, Y. Guo, X. Wang, Y. Tsujimoto, J. Li, S. Zhang, Y. Matsushita, Y. Shi, H. Tian, H. Yang, J. Li, and K. Yamaura, Superconducting and structural properties of δ-MoC$_{0.681}$ cubic molybdenum carbide phase, J. Sol. State Chem. **196**, 579 (2012).

[26] M. Žemlička, P. Neilinger, M. Trgala, M. Rehák, D. Manca, M. Grajcar, P. Szabó, P. Samuely, Š. Gaži, U. Hübner, V. M. Vinokur, and E. Il'ichev, Finite quasiparticle lifetime in disordered superconductors, Phys. Rev. B **92**, 224506 (2015).

[27] R. C. Dynes, V. Narayanamurti, and J. P. Garno, Direct Measurement of Quasiparticle-Lifetime Broadening in a Strong-Coupled Superconductor, Phys. Rev. Lett. **41**, 1509 (1978).

[28] A possible source can be a subnanometer normal metallic layer at the substrate-MoC interface similar to the case of thin Nb films [C. Delacour, L. Ortega, M. Faucher, T. Crozes, T. Fournier, B. Pannetier, and V. Bouchiat, Persistence of superconductivity in niobium ultrathin films grown on R-plane sapphire, Phys. Rev. B **83**, 144504 (2011)], in MoC due to, e.g., uncompensated orbitals.

[29] S. M. Hollen, G. E. Fernandes, J. M. Xu, and J. M. Valles, Collapse of the Cooper pair phase coherence length at a superconductor-to-insulator transition, Phys. Rev. B **87**, 054512 (2013).